Received July 1, 2020, accepted July 24, 2020, date of publication August 7, 2020, date of current version August 18, 2020.

Digital Object Identifier 10.1109/ACCESS.2020.3014904

Acceleration Slip Regulation of Distributed Driving Electric Vehicle Based on Road Identification

QIPING CHEN[1], SHENG KANG[1], HUI CHEN[1], YU LIU[1], AND JIE BAI[2]
[1]Key Laboratory of Conveyance and Equipment, Ministry of Education, East China Jiaotong University, Nanchang 330013, China
[2]School of Automotive Studies, Tongji University, Shanghai 201804, China

Corresponding author: Qiping Chen (qiping3846758@163.com)

This work was supported by the Foundation of Educational Department of Jiangxi Province under Grant GJJ190305.

ABSTRACT In order to eliminate excessive slip phenomenon of driving wheels during the driving process for distributed driving electric vehicle, an acceleration slip regulation strategy is analyzed and proposed. Based on Burckhardt tire model, a real-time road estimator is designed, which can obtain the current road attachment coefficient and the optimum slip rate. The torque fuzzy controller is designed, which can adjust the driving torque of each driving wheel. Then it comes to a better realization of the vehicle slip rate accurate control, and the slip rate of each driving wheel can be change within the optimum slip rate range. Study results indicate that the acceleration slip regulation strategy is an effective way to improve the dynamic performance and stability of the distributed driving electric vehicle in this paper.

INDEX TERMS Distributed driving electric vehicle, acceleration slip regulation, fuzzy control, road identification.

I. INTRODUCTION

Distributed drive is the ultimate driving mode of electric vehicle. Its main technical feature is that four in-wheel motors are used to driving the electric vehicle and the torque of each driving wheel can be controlled independently [1]. If the driving force of the left and the right wheel are imbalance during driving process, the vehicle will lose stability, especially when the vehicle is running on the low attachment coefficient road. Acceleration slip regulation is usually used to prevent the wheel from slipping in the process of accelerating [2]. To improve the power, stability and safety of distributed driving electric vehicle, it is necessary to control the driving wheel slip rate.

Acceleration slip regulation system has a great influence on the comprehensive performance of vehicles, and the control methods of acceleration slip regulation at home and abroad mainly include fuzzy control method, adaptive neural network control method, sliding mode control, and so on. Fu *et al.* [3] adopted proportional-integral-derivative (PID) algorithm to control the slip rate of vehicle driving wheel, and the simulation is carried out, but the adaptability of PID control is poor. Li *et al.* [4] simplified the fuzzy road identification method, and the acceleration slip regulation fuzzy PID controller for two rear-wheel independent drive micro-electric vehicle is designed, which can better restrain the excessive spinning of driving wheels. Feng *et al.* [5] proposed a control strategy of optimum slip rate, and the fuzzy controller controlled the motor torque. The control system adopts fixed optimum slip rate so that acceleration slip regulation cannot adapt to different roads. Hartani *et al.* [6] proposed a new longitudinal control strategy that combines Acceleration Slip Regulation (ASR) traction and Anti-lock Braking System (ABS) braking control, the motor torque and based on Fuzzy logic control, and the acceleration slip regulation is designed which can keep the wheel slip in the optimum range. Nam *et al.* [7] proposed a robust wheel slip control system based on sliding mode control, and verified the traction performance and effectiveness through field tests. Sharifi and Amirjamshidi [8] proposed a sliding control system by using of fuzzy to prevent wheel sliding in the situation of driver extreme brake or acceleration. Li *et al.* [9] designed an electric vehicle traction control system (TCS) based on sliding mode control, which is combined with optimum slip ratio estimation algorithm, and single road driving simulation is carried out.

The associate editor coordinating the review of this manuscript and approving it for publication was Feifei Bu.

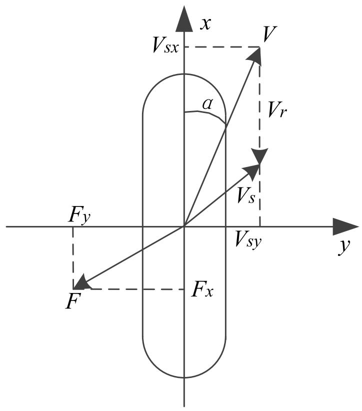

FIGURE 1. The forces and velocities of tire.

The research of Acceleration Slip Regulation is one of the urgencies in the process of developing the distributed driving electric vehicle. Therefore, an acceleration slip regulation strategy is presented in this paper. The distributed driving electric vehicle is simulated and analyzed by Carsim soft. The road estimator and slip rate control strategy are simulated and analyzed by Simulink soft, and the Co-simulation model is built to analyze the effectiveness of the acceleration slip regulation strategy.

II. ESTABLISHMENT OF VEHICLE MODEL

A. ESTABLISHMENT OF TIRE MODEL

There are longitudinal slip and lateral slip between tire and road surface in the actual driving conditions of vehicle. It is necessary to analyze the forces and velocities of vehicle tire under longitudinal-lateral coupling conditions [9]. The forces and velocities of tire are shown in FIGURE 1.

As shown in FIGURE 1, the longitudinal velocity of the contact point on the ground mark relative to wheel center is shown in Formula (1).

$$\mathrm{V}_r = \omega \cdot r \tag{1}$$

where, ω is the angular speed of wheel, r is the wheel radius. The lateral and longitudinal slip velocities of the contact point on the ground mark relative to road surface are shown in Formula (2).

$$\begin{cases} V_{sx} = V \cdot \cos\alpha - V_r \\ V_{sy} = V \cdot \sin\alpha \end{cases} \tag{2}$$

where, V_{sx} is the lateral slip velocity of the contact points on the ground mark relative to the road surface, V_{sy} is the longitudinal slip velocity of the contact points on the ground mark relative to the road surface, V is wheel speed, α is the angle between wheel speed and the rotation plane of wheel.

Wheel slip rate can be calculated by Formula (3).

$$S = \sqrt{\left(\frac{(\omega r - v_{sx})}{v_{sx}}\right)^2 + \left(\frac{v_{sy}}{v_{sx}}\right)^2} \tag{3}$$

where, $V_s = [v_{sx} - \omega r, v_{sy}]^T$, $V = [v_{sx}, v_{sy}]^T$.

B. ESTABLISHMENT OF IN-WHEEL MOTOR MODEL

Distributed driving electric vehicle is driving by permanent magnet synchronous motors (PMSM), so it is necessary to establish a mathematic model of PMSM. The driving motor is modeled according to the principle of vector control, which can simplify the process of model building [11]. A mathematic model of PMSM in $d - q$ coordinate system is built. The stator voltage is shown in Formula (4).

$$\begin{cases} u_d = Ri_d + L_s\dfrac{di_d}{dt} - p_n\omega_m L_s iq \\ u_q = Ri_q + L_s\dfrac{di_q}{dt} + p_n\omega_m L_s i_d + pn\omega m\varphi f \end{cases} \tag{4}$$

where, R is the stator resistance, i_d is the electric current of d axis, i_q is the electric current of q axis, L_s is the stator inductance, p_n is the number of pole pairs, ω_m is the electric angular velocity of motor, and φ_f is the permanent magnet flux linkage.

The electromagnetism torque of permanent magnet synchronous motor is shown in Formula (5).

$$T_e = \frac{3}{2}p_n[i_q\varphi_f + i_d i_q(L_d - L_q)] \tag{5}$$

where, L_d is the inductance of d axis, and L_q is the inductance of q axis.

The motion equation of permanent magnet synchronous motor is shown in Formula (6).

$$J\frac{d\omega m}{dt} = Te - TL - B\omega m \tag{6}$$

where, J is the moment of inertia, B is the damping coefficient, and T_L is the load torque.

This paper has adopted the control technique of the rotor flux orientation, which can obtain better control effect [12]. The stator voltage, electromagnetism torque and motion equation of PMS motor are redefined respectively, as shown in Formula (7), (8) and (9).

$$\begin{cases} ud = -pn\omega mLsiq \\ uq = Riq + Ls\dfrac{diq}{dt} + pn\omega m\varphi f \end{cases} \tag{7}$$

$$T_e = \frac{3}{2}pniq\varphi f \tag{8}$$

$$J\frac{d\omega m}{dt} = Te - TL - B\omega m \tag{9}$$

According to above analysis, the mathematic model of permanent magnet synchronous motor is deduced, and the relevant motor module is established by 1-D lookup table module in Simulink.

III. ROAD IDENTIFICATION ALGORITHMS

The purpose of acceleration slip regulation is to keep the slip rate of wheels under optimal state, so it is necessary to obtain the road attachment coefficient and optimum slip rate. The average attachment coefficient of typical road [13] is shown in TABLE 1.

TABLE 1. Average attachment coefficient of typical road [13].

Road	Peak Adhesion Coefficient	Optimum slip rate
Asphalt (dry)	0.8~0.9	0.17
Asphalt (wet)	0.5~0.7	0.13
Gravel(wet)	0.6	0.14
Snow (compress)	0.2	0.06
Ice	0.1	0.03

Burckhardt tire model better describes the relationship between slip rate and tire longitudinal force [13]. Burckhardt tire model can be expressed by Formula (10).

$$\mu = \theta_1 - \theta_1 \exp(-\frac{\theta_2}{\theta_1}(S + C_5 S^2)) - C_3 S + C_4 S^2 \quad (10)$$

where, μ is the utilization of adhesion coefficient, θ_1 is the peak attachment coefficient of road, θ_2 is the Longitudinal sliding stiffness, C_3, C_4 and C_5 are the shape parameters of longitudinal tire force and wheel slip rate curve.

Fit the value of C_3, C_4, C_5 through tire test, integrated the tire model is into the standard calculation flow of Levenberg Marquardt algorithm. According to the tire model expression, the parameters to be evaluated are recorded as X_1, X_2, and the slip ratio is recorded as S, as shown in Formula (11).

$$\mu(S, X_1, X_2) = X_1 - X_1 \exp[-\frac{X_2}{X_1}(S + C_5 S^2)] - C_3 S \operatorname{sgn}(S) + C_4 S^2 \quad (11)$$

The expression of residual $f(x)$ is shown in Formula (12).

$$f(x) = \begin{bmatrix} \tilde{\mu}_1 - \mu(x, S_1) \\ \cdots \\ \tilde{\mu}_{Npnt} - \mu(x, S_{Npnt}) \end{bmatrix} \quad (12)$$

where, $\tilde{\mu}_{Npnt}$ and S_{Npnt} are a set of sampling information of adhesion rate and slip rate.

Jacobian matrix $J(x)$ is shown in Formula (13).

$$J(x) = \begin{bmatrix} \frac{\partial \mu}{\partial X_1}(x) \\ \frac{\partial \mu}{\partial X_2}(x) \end{bmatrix}^T \quad (13)$$

Formula (14) can express the single wheel mathematic model.

$$I_w \dot{\omega} = T - F_x R = T - F_z \mu R \quad (14)$$

When obtained tire longitudinal force then the utilization of attachment coefficient can be calculated by Eq. (14). As the value of C_3, C_4 and C_5 does not change much, and the tire characteristic is insignificant influenced by θ_2. The value of θ_1 can be easily obtained, as the parameters of C_3, C_4, C_5 and θ_2 be set to empirical values [15]. The optimum slip rate is obtained by the 1-D look up table.

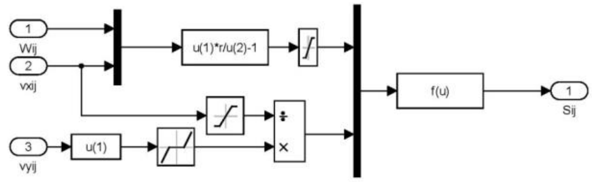

FIGURE 2. Slip rate computation module.

TABLE 2. Control rules of fuzzy controller [5].

Slip error (e)	Change rate of slip rate error (ec)		
	NB	Z	B
N	N	N	N
ES	Z	Z	S
S	Z	S	S
M	S	M	B
B	M	B	EB

IV. ESTABLISHMENT OF SIMULATION MODEL

A. SLIP RATE COMPUTATION MODULE

According to Eq. (3), the slip rate computation module is shown in FIGURE 2, ω_{ij} is the angular speed of each wheel, v_{xij} is the longitudinal speed of each wheel, and v_{yij} is the lateral speed of each wheel.

B. DRIVING TORQUE ADJUSTMENT MODULE

Fuzzy control algorithm can regulate the driving torque of each wheel. The slip error and the change rate of slip rate error are regarded as the inputs of wheel torque fuzzy controller [16]. The slip error (e) of wheel slip rate S_{ij} and optimum slip rate S_{oij} is taken five fuzzy subsets, which are N(negative), ES (extremely small), S(small), M(middle) and B(big) respectively. The change rate of slip rate error (ec) is taken three fuzzy subsets, which are NB (negative big), Z(zero) and B(big). Control torque T_{c_ij} is taken six fuzzy subsets, which are N(negative), Z(zero), S(small), M(middle), B(big) and EB (extremely big). In order to keep the driving torque from fluctuating greatly, the membership functions of input and output variables are all Gaussian membership functions [17]. The control rules of fuzzy controller are expressed in TABLE 2.

The membership function of inputs and outputs of torque fuzzy controller is expressed in FIGURE 3.

C. SLIP RATE CONTROL STRATEGY

The structure of slip rate control strategy is shown in FIGURE 4. FIGURE 4 indicates that the driver presses the accelerator pedal to input the throttle signal to the distributed drive electric vehicle. The road identification module obtained the optimum slip rate of the current driving road by the wheel torque, wheel longitudinal force, wheel vertical force and wheel angular acceleration information. The slip rate computation module calculates the wheel slip rate by

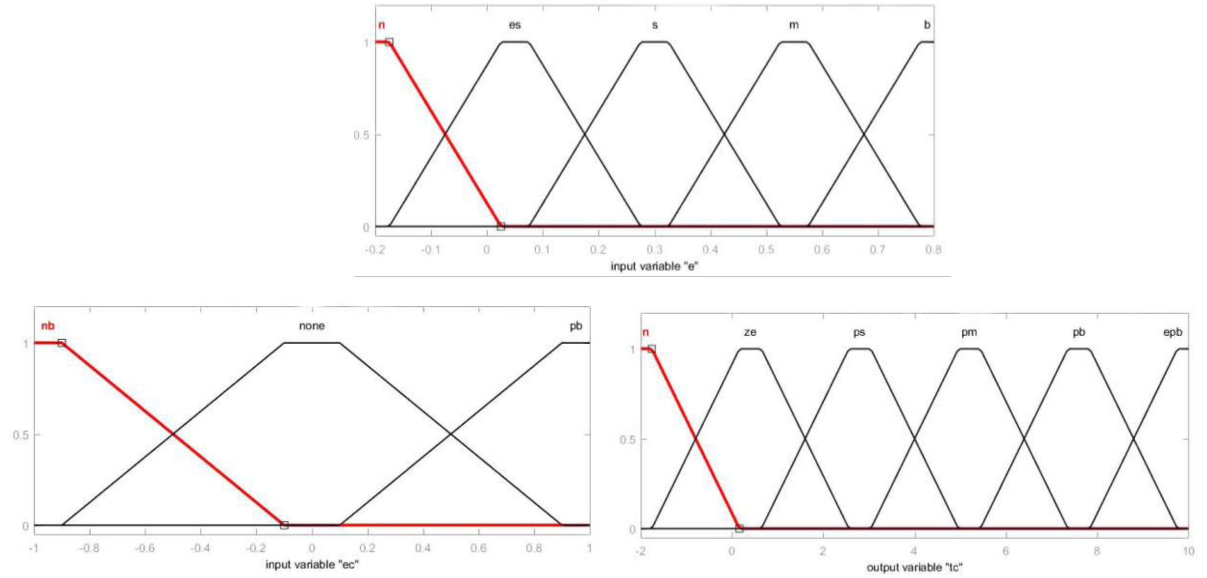

FIGURE 3. Membership function of inputs and outputs of torque fuzzy controller.

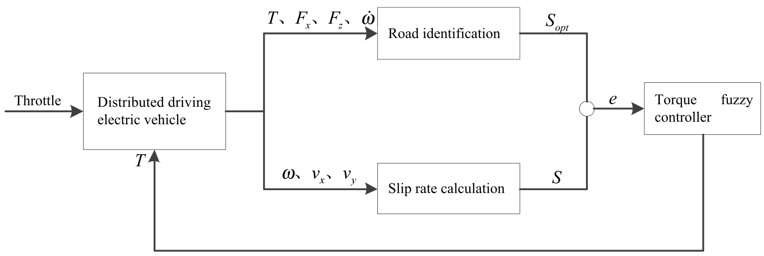

FIGURE 4. Structure of slip rate control strategy.

TABLE 3. Main vehicle parameters.

Parameter	Value
Mass / kg	1381
Tire size	185/65
Wheelbase / m	2.30
Rolling radius / m	0.29
Distance between COG and Front axle/ m	1.12
Distance between COG and Rear axle / m	1.18

wheel angular, vehicle longitudinal and lateral speed. Then the torque fuzzy controller adjusts the driving torque by the slip rate error.

V. SIMULATION AND ANALYSIS

A distributed driving electric vehicle model is established by Carsim. The main parameters of the vehicle are shown in TABLE 3.

Because there is no motor model in Carsim, the external in-wheel motor model is used to provide driving torque in the power transmission part. The vehicle model in Carsim is combined with the in-wheel motor model, the slip rate computation module, the road identification module and the acceleration slip regulation system established by Simulink. The specific Co-simulation computation model is expressed in FIGURE 5.

A. LOW ATTACHMENT COEFFICIENT ROAD DRIVING

This paper has established the road with attachment coefficient by Carsim soft, which can be used to verify the validity of slip rate computation module, road identification module and acceleration slip regulation strategy. The vehicle is start-up from stop and the throttle is ramp to full in 0.1s. The joint simulation experiment is carried out.

Wheel slip rate on low attachment coefficient road is shown in FIGURE 6, where slip rate fl is the slip rate of front left wheel, slip rate fr is the slip rate of front right wheel, slip rate rl is the slip rate of rear left wheel and slip rate rr is the slip rate of rear right wheel. As shown in FIGURE 6, in the process of throttle opening increasing from 0 to 1,

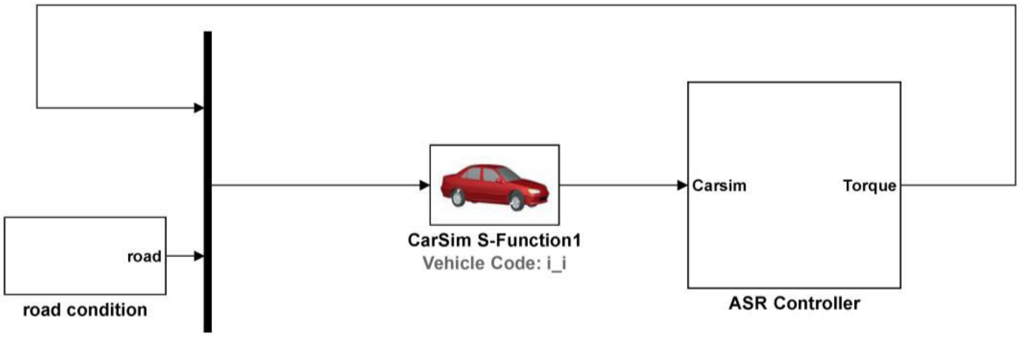

FIGURE 5. Co-simulation computation model.

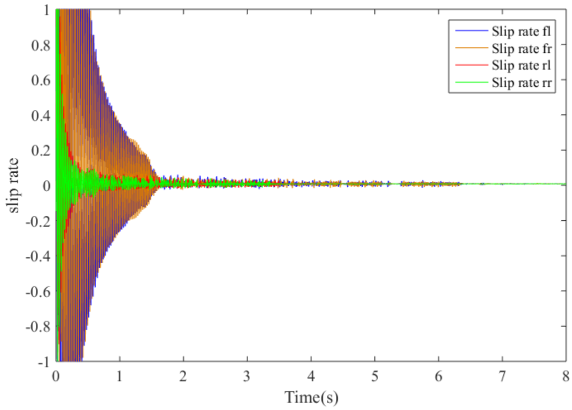

FIGURE 6. Wheel slip rate on low attachment coefficient road.

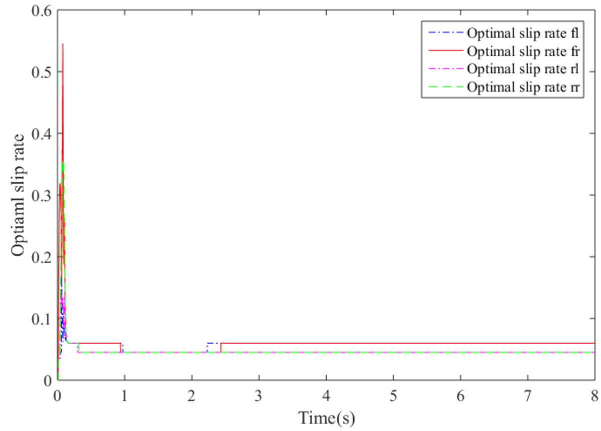

FIGURE 7. Optimum slip rate on low attachment coefficient road.

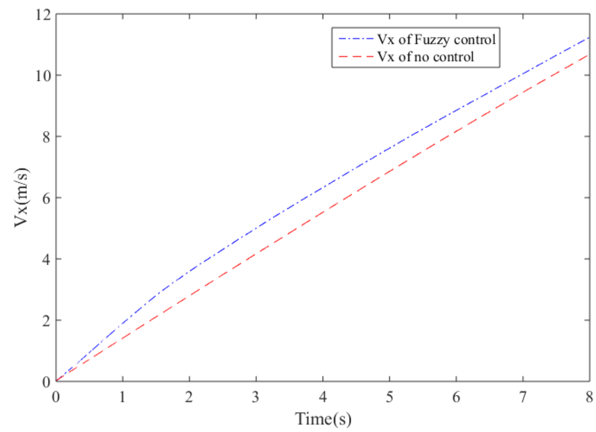

FIGURE 8. Velocity of vehicle on low attachment coefficient road.

vehicles start from stop. The change rate of four-wheel slip rate difference varies greatly, and the slip rate of four wheels reaches a stable state after vehicle start at 1.6s. The slip rate of front right wheel and rear wheel all near 0.008 and the slip rate of front wheels fluctuate steadily from −0.01 to 0.03 before 6.35 s. After 6.35 s, the slip rate of front wheel decreases gradually, and eventually it is the same as rear wheels. From the wheel slip rate on low attachment coefficient road curve, it is easy to know that acceleration slip regulation strategy can better maintain the wheel without slip phenomenon in vehicle running process.

Optimum slip rate on low attachment coefficient road is shown in FIGURE 7. As shown in FIGURE 7, optimum slip rate fl is the optimum slip rate of front left wheel, optimum slip rate fr is the optimum slip rate of front right wheel, optimum slip rate rl is the optimum slip rate of rear left wheel and optimum slip rate rr is the optimum slip rate of rear right wheel. In the process of throttle opening increasing from 0 to 1, vehicles start from stop. The value of optimum slip rate of four-wheel increases rapidly from zero, and the amplitude of optimum slip rate is 0.545. During vehicle starting stage, slip rate varies greatly and the peak attachment coefficient estimated by road estimator is smaller, which leads to the optimum slip rate exceeds 0.2. The optimum slip rate decreases rapidly after reaching the amplitude, the optimum slip rate of rear wheels reaches to the steady value of 0.045 at 0.31 s, and the optimum slip rate of front wheels reaches to the steady value of 0.06 at 2.4s. From the optimum slip rate on low attachment coefficient road curve, it is easy to know that the slip rate computation module and the road identification module can identify the road conditions rapidly, and the optimum slip rate can be obtained according to the wheel slip rate quickly.

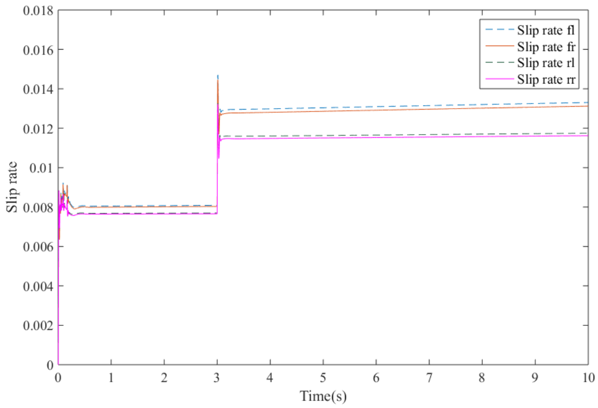

FIGURE 9. Wheel slip rate on docking road.

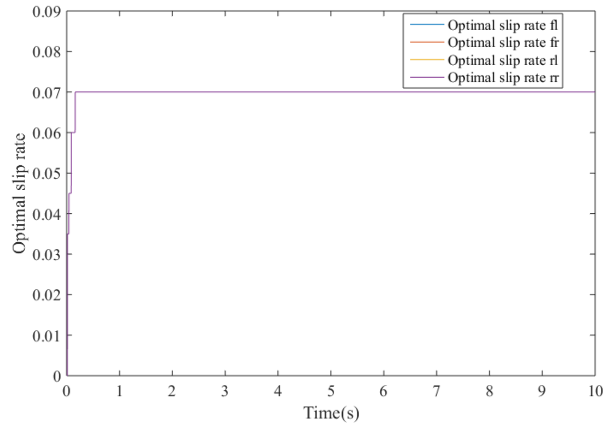

FIGURE 10. Optimum slip rate on docking road.

Velocity of vehicle on low attachment coefficient road is shown in FIGURE 8. As shown in FIGURE 8, the velocity growth of vehicle under Fuzzy control is faster. The velocity growth of Fuzzy control and no control is seeming to equal before 0.31 s, as for the acceleration slip regulation module limits the velocity growth rate to prevent the slip rate from changing greatly. The optimum slip rate reaches to stability value in about 0.31 s, so that the growth rate of vehicle speed is relatively faster after 0.31 s, and velocity of vehicle finally reaches to 11.24 m/s.

B. DOCKING ROAD DRIVING

The docking road is established in this paper, which can further verify the effectiveness of the acceleration slip regulation strategy. The first attachment coefficient is 0.6, and the second is 0.2. The original speed of vehicle is 50 km/h, and the throttle is ramp to full in 0.1 s. The relevant simulation results are obtained as follow.

Wheel slip rate on docking road is shown in FIGURE 9. As shown in FIGURE 9, the slip rate of four-wheel is near 0.008, and the slip rate of left and right wheel of front and rear is same. The slip rate of front wheels increases to 0.0128, and the rear wheels increases to 0.0115 after 3 s. The change trend of wheel slip rate of on docking road is not similar to the wheel slip rate on low attachment coefficient road, the change frequency of each wheel is smaller, and the slip rate of four-wheel fluctuates tinily when it reaches steady state. From the curve of wheel slip rate on docking road, it is easy to know that when vehicle running on different roads, the acceleration slip regulation strategy still can keep the wheel slip rate in a small range.

Optimum slip rate on docking road is shown in FIGURE 10. As shown in FIGURE 10, in the process of throttles opening increasing from 0 to 1. The optimum slip rate of four-wheel increases rapidly from zero, the optimum slip rate of four-wheel reaches the steady value of 0.07 at 0.162 s.

Velocity of vehicle on docking road is shown in FIGURE 11. FIGURE 11 indicates that the vehicle velocity

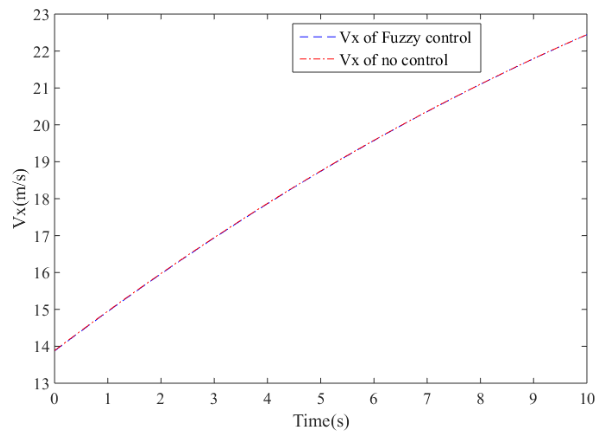

FIGURE 11. Velocity of vehicle on docking road.

under Fuzzy control is equal. The driving torque of four-wheel also can reache to steady value quickly, as for vehicle has an original speed velocity of 50 km/h, the slip rate of four-wheel and the optimum slip rate reaches to steady value quickly. Above such reasons the velocity of Fuzzy control and no control is equal, and velocity of vehicle finally reaches to 22.5 m/s.

VI. CONCLUSION

1) The acceleration slip regulation strategy and the optimum slip rate identification based on Fuzzy control are designed, and wheel longitudinal and lateral slip rate are considered in the calculation of wheel slip rate. The co-simulation of low attachment coefficient road and docking driving for distributed driving electric vehicle were carry out by Carsim and Simulink. The co-simulation of low attachment coefficient road and docking driving for distributed driving electric vehicle were carry out by Carsim and Simulink.

2) The study results indicate that the optimum slip rate identification module can obtain wheel slip rate and optimum slip rate better on different road. The acceleration slip regulation strategy can maintain wheel slip rate of distributed driving vehicle in a lower range, which is an effective way

to improve the dynamic performance and stability of the distributed driving electric vehicle.

3) The fluctuation of wheel slip rate is greater during initial driving stage on low attachment coefficient road, and the accuracy of the optimum slip rate of variable road estimation by road identification module should be improved. Therefore, the next work of this paper is to solve the excessive problem of slip rate in low speed start stage, and improve the adaptability and accuracy of road identification module.

ACKNOWLEDGMENT

The authors would like to thank anonymous reviewers for their helpful comments and suggestions to improve the manuscript.

REFERENCES

[1] N. Mutoh, "Driving and braking torque distribution methods for front- and rear-wheel-independent drive-type electric vehicles on roads with low friction coefficient," *IEEE Trans. Ind. Electron.*, vol. 59, no. 10, pp. 3919–3933, Oct. 2012.
[2] M. V. Butz and T. D. Lonneker, "Optimized sensory-motor couplings plus strategy extensions for the TORCS car racing challenge," in *Proc. IEEE Symp. Comput. Intell. Games*, Sep. 2009, pp. 317–324.
[3] Q. Fu, L. Zhao, X. Sun, M. Cheng, and M. Cai, "Study on anti-slip regulation of quarter automobile based on PID control," in *Proc. 2nd Int. Conf. Consum. Electron., Commun. Netw. (CECNet)*, Apr. 2012, pp. 2111–2114.
[4] Z. Li, S. Hou, and H. Li, "Acceleration slip regulation of mini electric vehicle with in-wheel motors," *J. Hebei Univ.*, vol. 37, no. 3, pp. 322–328, 2017.
[5] Y. Feng, J. Yang, Z. Ji, and W. Zhang, "Fuzzy anti-slip control based on optimal slip control," *Trans. Chin. Soc. Agricult. Eng.*, vol. 31, no. 8, pp. 119–125, 2015.
[6] K. Hartani, M. Khalfaoui, A. Merah, and N. Aouadj, "A robust wheel slip control design with radius dynamics observer for EV," *SAE Int. J. Vehicle Dyn., Stability, NVH*, vol. 2, no. 2, pp. 135–146, Jun. 2018.
[7] K. Nam, Y. Hori, and C. Lee, "Wheel slip control for improving traction-ability and energy efficiency of a personal electric vehicle," *Energies*, vol. 8, no. 7, pp. 6820–6840, Jul. 2015.
[8] J. Sharifi and A. Amirjamshidi, "Fuzzy electronic stability control system for electric vehicle with four motor in wheel," *J. Control*, vol. 9, no. 4, pp. 41–53, 2016.
[9] X. Li, L. He, W. Ye, and M. Hu, "Design of the sliding mode controller of TCS for electric vehicle," *Comput. Simul.*, vol. 37, no. 2, pp. 144–148 and 230, 2020.
[10] Z. Yu, L. Gao, R. Zhang, and L. Xiong, "Dynamic control of electric motor driven skid steered vehicles," *J. Tongji Univ.*, vol. 46, no. 5, pp. 631–638, 2018.
[11] Y. A.-R.-I. Mohamed, "Design and implementation of a robust current-control scheme for a PMSM vector drive with a simple adaptive disturbance observer," *IEEE Trans. Ind. Electron.*, vol. 54, no. 4, pp. 1981–1988, Aug. 2007.
[12] A. M. Aljehaimi and P. Pillay, "Online rotor flux linkage estimation for a variable flux interior permanent magnet syncronous machine operating at different flux density levels," in *Proc. IEEE Int. Conf. Power Electron., Drives Energy Syst. (PEDES)*, Dec. 2016, pp. 1–6.
[13] M. Duan, W. Guo, and G. Li, "Study on acceleration slip regulation control of electric vehicle with two independent drive wheels," *J. Liaoning Inst. Technol.*, vol. 36, no. 4, pp. 257–261, 2016.
[14] T. K. Bera, K. Bhattacharya, and A. K. Samantaray, "Evaluation of antilock braking system with an integrated model of full vehicle system dynamics," *Simul. Model. Pract. Theory*, vol. 19, no. 10, pp. 2131–2150, Nov. 2011.
[15] X. Wang, H. Wang, X. Chen, and D. Qi, "Simulation of field oriented control of hub motor," *Comput. Simul.*, vol. 34, no. 9, pp. 141–145 and 198, 2017.
[16] A. Harifi, A. Aghagolzadeh, G. Alizadeh, and M. Sadeghi, "Designing a sliding mode controller for slip control of antilock brake systems," *Transp. Res. C, Emerg. Technol.*, vol. 16, no. 6, pp. 731–741, 2008.
[17] D. K. Sambariya and R. Prasad, "Selection of membership functions based on fuzzy rules to design an efficient power system stabilizer," *Int. J. Fuzzy Syst.*, vol. 19, no. 3, pp. 813–828, 2017.

QIPING CHEN received the Ph.D. degree in mechanical engineering from Chongqing University, Chongqing, China, in 2013. He is currently an Associate Professor with the Key Laboratory of Conveyance and Equipment, Ministry of Education, East China Jiaotong University, China. He is the sponsor and instructor of this article. His research interests include electric vehicles, hybrid vehicles, and mechatronics.

SHENG KANG is currently pursuing the M.S. degree with the Key Laboratory of Conveyance and Equipment, Ministry of Education, East China Jiaotong University, China. He is responsible for the writing and model building of this article. His research interests include vehicle dynamics and electric drive control.

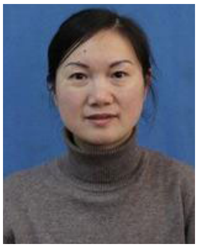

HUI CHEN received the M.S. degree in mechanical engineering from East China Jiaotong University, China, in 2004. She is currently an Associate Professor with the School of Mechatronics and Vehicle Engineering, East China Jiaotong University. She is the assistant of model building in this article. Her research interests include electric vehicles, hybrid vehicles, and mechatronics.

YU LIU is currently pursuing the M.S. degree with the Key Laboratory of Conveyance and Equipment, Ministry of Education, East China Jiaotong University, China. He is the translator of this article. His research interests include electric vehicles and EHB.

JIE BAI received the Ph.D. degree in mechanics of materials from Hiroshima University, Hiroshima, Japan, in 1996. He is the Chief Scientist of intelligent vehicle environment comprehensive perception systems with Tongji University, China. He is the proofreader of this article. His research interests include automobile environment perception, information fusion technology, and intelligent automobile technology.